Research Square

Preprints are preliminary reports that have not undergone peer review.
They should not be considered conclusive, used to inform clinical practice,
or referenced by the media as validated information.

Consistency of the seismic zonation proposed for the Greek National Annex to EC8-2G with the Annex F near-collapse reliability target: a risk-targeting check using ESHM20

Alexandros Lalas

a.lalas@archirodon.net

Archirodon N.V.

Case Report

Keywords: Eurocode 8, seismic zonation, risk targeting, near-collapse limit state, ESHM20, Greece

Posted Date: November 17th, 2026

DOI: https://doi.org/10.21203/rs.3.rs-11509817/v1

License: This work is licensed under a Creative Commons Attribution 4.0 International License.
Read Full License

Additional Declarations: No competing interests reported.

Consistency of the seismic zonation proposed for the Greek National Annex to EC8-2G with the Annex F near-collapse reliability target: a risk-targeting check using ESHM20

Alexandros Lalas[1,*]

Abstract

A proposed Greek National Annex to the second-generation Eurocode 8 (EC8-2G) would replace the three-zone map of EAK 2003 with five zones derived from the European Seismic Hazard Model ESHM20, assigning each zone the average median $S_{\alpha,475}$ and 84th-percentile $S_{\beta,475}$ of its grid points. The zonation is tested against the Annex F reliability target for near collapse (NC) in consequence class CC2 (2×10^{-4}/yr). Lognormal NC fragilities are anchored to the code demand and calibrated so that the target is met exactly where the median hazard follows the code's power law with slope k=3; the ratio of the annual NC probability to the target, P_{NC}/P_t, therefore measures departure from the code's idealisation, not the collapse probability of real buildings. Rock hazard curves are integrated at 59 cities and 55 Athens municipal units. On the median hazard used by Annex F, structures with fundamental period T_1 of about 0.1–0.2 s lie at 0.62–2.06 times the target (population-weighted 1.21) and structures with T=1 s at 0.20–1.23 times (0.69); on the mean hazard, 1.96 and 0.86. Across the plateau, P_{NC} falls from 1.41 times the target at the spectral peak to 0.61 at the corner period. The mixed percentile convention makes structures near the peak about twice as likely to exceed NC as those at 1 s. Zone averaging changes P_{NC} approximately as $(1+r)^{-2.7}$, r being the zone-to-site deviation. Zone factors meeting the target are derived.

[1] Archirodon N.V., Athens, Greece.

ORCID: https://orcid.org/0000-0001-9483-6252

[*] Corresponding author. E-mail: a.lalas@archirodon.net

Keywords: Eurocode 8, seismic zonation, risk targeting, near-collapse limit state, ESHM20, Greece

1 Introduction

The second generation of Eurocode 8 (EC8-2G; EN 1998-1-1:2024, CEN 2024) anchors the elastic response spectrum to two hazard parameters: S_α, the spectral acceleration of the constant-acceleration plateau, and S_β, the spectral acceleration at $T_\beta = 1$ s (Labbé and Paolucci 2022). National Annexes provide their values for the reference return period of 475 years, either on a dense grid or grouped into seismic zones (EN 1998-1-1, 5.2.1). EC8-2G also relates the seismic action to target reliability indices given in its informative Annex F. The return periods of the limit states follow from these indices, and so do the performance factors that may replace the return periods (4.3; Franchin and Noto 2023).

For Greece, Pitilakis et al. (2024) proposed a five-zone map based on ESHM20 (Danciu et al. 2021, 2024) to replace the three-zone map of the 2003 Greek seismic code (EAK 2003). According to announcements in the public media, at the time of writing (October 2026) the proposal, with a draft National Annex, has

been submitted to the Greek Earthquake Planning and Protection Organization (OASP) and the national standards body (ELOT), and is under consideration. Zone boundaries follow the median $S_{\alpha,475}$. Each zone is assigned the average of the median $S_{\alpha,475}$ of its grid points and the average of the 84th-percentile $S_{\beta,475}$. The higher percentile for S_β was chosen because median values give a narrow plateau and lower design forces for typical 3–8-storey buildings. The zonation was accepted when the zone peak ground acceleration (PGA) deviated from the ESHM20 value at each test city by less than a population-dependent threshold: $\pm 20\%$ up to 100,000 inhabitants, $\pm 15\%$ up to 500,000 and $\pm 10\%$ above that.

This criterion measures how faithfully the zonation reproduces the ESHM20 hazard at 475 years, not the reliability that results from designing to it. Uniform-hazard design does not give uniform risk, because the slope and curvature of hazard curves vary between sites (Luco et al. 2007); this is the basis of risk-targeted design maps (Douglas et al. 2013; Silva et al. 2016; Gkimprixis et al. 2019; Žižmond and Dolšek 2019; Monti et al. 2023; Spillatura et al. 2023). Zoning adds a second source of non-uniformity (averaging), and the use of different percentiles for S_α and S_β adds a third source of non-uniformity.

The relations used (the closed-form risk integral of Cornell et al. 2002 and the power-law scaling of risk with design intensity) are standard; the contribution is their application to an EC8-2G national zonation against the code's own target. This study asks how far the zone values depart from the target and why, how the hazard tolerance of the zonation translates into risk, what the percentile convention and the Zone 1 value of 0.13 g (PGA on rock) imply, and which zone factors would meet the target.

2 Data and method

2.1 Sites, zones and population

The sample comprises the test cities of Pitilakis et al. (2024), each assigned the zone listed for it in their appendix and that zone's $S_{\alpha,475}$ and $S_{\beta,475}$ (Table 1) at city-centre coordinates. Their text refers to 61 cities, but their appendix lists 60, without Piraeus. Because the zoning proposal divides the Athens region between zones, Athens is represented by the 55 municipal units of the four Athens regional units and Piraeus (the Athens urban area), which leaves 59 cities. The zones of these units are read from the georeferenced zone map (Pitilakis et al. 2024); the same procedure reproduces the tabulated zone of all 60 cities. Of the Athens units, 53 lie in Zone 2; Petroupoli and Kamatero, on the Zone 2/3 boundary, are assigned Zone 3 (Online Resource 1).

Populations are ELSTAT 2021 figures (Hellenic Statistical Authority 2023) for the units used by Pitilakis et al. (2024). The 114 sites hold 6.0 million people, 57% of the national population, half of them in the Athens urban area. Unweighted statistics treat the Athens urban area as one site, the population-weighted aggregate of its 53 Zone 2 units (60 sites). Population serves only to weight sites against one another; it is not the number of occupants of buildings designed to the new code.

Table 1 Proposed zone values on rock (Pitilakis et al. 2024), sites and 2021 population of the main sample, and population-weighted P_{NC}/P_t under zone design on the ESHM20 median hazard (mean hazard in brackets). Ranges are minimum–maximum over the sites of each zone. Code-calibrated fragility, $\beta = 0.6$, rock.

Zone	$S_{\alpha,475}$ (g)	$S_{\beta,475}$ (g)	PGA (g)	Sites	Population	P_{NC}/P_t short-period	P_{NC}/P_t intermediate-period
1	0.32	0.13	0.13	4	211,247	1.69 (1.27–2.06) [2.35]	0.72 (0.47–0.84) [0.97]
2	0.47	0.15	0.19	11 + 53	3,398,751	1.30 (0.85–2.00) [2.04]	0.77 (0.44–1.09) [0.92]
3	0.58	0.18	0.23	7 + 2	1,121,870	1.01 (0.90–1.19) [1.79]	0.60 (0.37–0.80) [0.80]
4	0.73	0.25	0.29	26	898,041	1.07 (0.62–1.53) [1.69]	0.62 (0.29–1.23) [0.79]
5	0.93	0.34	0.37	11	377,066	1.06 (0.66–1.90) [2.06]	0.38 (0.20–0.68) [0.59]
All				114	6,006,975	1.21 (0.62–2.06) [1.96]	0.69 (0.20–1.23) [0.86]

Sites: cities + Athens urban-area units.

2.2 ESHM20 hazard curves

Rock hazard curves (V_{S30} = 800 m/s) for PGA and spectral accelerations of 0.05–1.0 s, for the mean and the 5th to 95th percentiles, were retrieved from the European Facility for Earthquake Hazard and Risk (EFEHR) web service (Danciu et al. 2021) at the four ESHM20 grid nodes (0.1° spacing) surrounding each site, converted to annual rates and interpolated bilinearly in log rate. Above the highest intensity level (3–5 g) the curves are extrapolated along their last log–log segment; replacing the extrapolation by zero changes P_{NC} by at most 0.6% on the median hazard and 3.3% on the mean.

2.3 Intensity measures

Following the definition of the ESHM20 S_α maps (Labbé and Paolucci 2022; Pitilakis et al. 2024), the period T_p of the peak of the median 475-year uniform hazard spectrum (UHS) is identified at each site. It is 0.15 s at 49 of the 59 cities and at all Athens units, and 0.20 s at 10 cities. The hazard curve of S_α is built by averaging the UHS over $[0.5T_p, 1.5T_p]$ at each annual rate λ. UHS ordinates between the computed periods are interpolated linearly in T:

$$S_\alpha(\lambda) = \frac{1}{T_p}\int_{0.5T_p}^{1.5T_p} \mathrm{UHS}\,(T;\lambda)\,dT \qquad (1)$$

Because averaging quantiles at a fixed rate assumes full correlation across periods, Eq. (1) is checked against hazard curves of SA(T_1) for T_1 = 0.10 s, T_p, 0.30 s and the zone corner period T_C (Sect. 3.2). Intermediate-period structures, on the constant-velocity branch of the spectrum, are represented by SA(1.0 s), the definition of S_β, with SA(0.5 s) and SA(0.75 s) as checks. The median $S_{\alpha,475}/2.5$ reproduces the city PGA values listed by Pitilakis et al. (2024) with a mean bias of +0.004 g.

2.4 Risk integral and code-calibrated fragility

The annual probability of exceeding NC is the risk integral of Annex F (Formula F.2):

$$P_{NC} = \int_0^{\infty} \lambda_H(c)\, f_C(c)\, dc \qquad (2)$$

Here f_C is the lognormal density of the NC capacity, with median θ and logarithmic standard deviation β. λ_H is the hazard function, which Annex F defines as "the median of annual frequency of exceedance" (F.4(2)). The median is anchored to the EC8-2G NC demand:

$$\theta = m\,\gamma_{NC}\,S_{475,zone}, \qquad S_{475,zone} = S_{\alpha,475} \text{ or } S_{\beta,475}\,T_\beta/T \qquad (3)$$

$\gamma_{NC} = 1.5$ is the performance factor for CC2, nominally a 1600-year action (4.3(5)). $S_{\beta,475}T_\beta/T$ is the design ordinate on the descending branch, $T \geq T_C$. On rock $F_\alpha = F_\beta = 1$. The margin m is the ratio of median NC capacity to NC demand. It combines all sources of margin between the two: material and system overstrength, the partial factors on resistance and the conservatism of the verification rules. The behaviour factor is not a margin in itself, since the strength reduction it allows is offset by the ductility verified at NC.

For CC2 the target is $P_t = 2.0 \times 10^{-4}$/yr ($\beta_t = 2.33$ in 50 years; EN 1998-1-1, Annex F). Annex F gives $\beta = 0.60$ for $T_1 \geq T_B$, decreasing to 0.40 at $T = 0$. The margin is calibrated so that a structure designed to S_{475} exactly meets P_t at a site whose median hazard is the power law of Formula F.4 with slope $k = 3$ through S_{475} at $T_{ref} = 475$ years. Substituting $\lambda_H(\theta) = (\theta/S_{475})^{-k}/T_{ref}$ into Formula F.5, $P_{NC} = \lambda_H(\theta)\exp(k^2\beta^2/2)$, and setting $P_{NC} = P_t$ gives

$$m_{EC8} = \frac{1}{\gamma_{NC}}\left[\frac{\exp(k^2\beta^2/2)}{T_{ref}\,P_t}\right]^{1/k} \qquad (4)$$

which is 2.51 for $\beta = 0.6$. By construction, $P_{NC}/P_t = 1$ at any site whose median hazard is a $k = 3$ power law through S_{475}. Every departure from 1 therefore comes from hazard-curve shape, zone averaging, the design fractile, or the use of the mean instead of the median hazard. P_{NC}/P_t is an index of the departure from the code's idealisation, not an estimate of the NC probability of actual buildings. The margin m is a calibration constant derived from the Annex F formulas; it is not derived from, or compared with, the partial factors of the material parts. As the calibration links m and β, the relative results change little with this choice (Sect. 3.2).

Equation (2) is integrated numerically in $\ln c$ over $\pm 7\beta$ with log–log interpolation of the hazard curve; an independent summation agrees within 1%.

Results are given on the median hazard, as Annex F specifies, and on the ESHM20 mean hazard as a sensitivity. Because Eq. (2) is linear in λ_H, the mean hazard gives the mean P_{NC} over the logic tree. The median hazard does not give the median P_{NC}. To separate zoning from uniform-hazard design itself, each

site is also evaluated with its own 475-year value under the same convention (median S_α, 84th-percentile S_β); this is called own-value design.

3 Results

3.1 Departure from the Annex F target

Figure 1 and Table 1 show P_{NC}/P_t under zone design. On the median hazard, short-period structures represented by the S_α construct, i.e. with T_1 of about 0.1–0.2 s (Sect. 3.2), lie between 0.62 (Limnos) and 2.06 (Drama) times the target, with a population-weighted mean of 1.21. The target is exceeded at sites holding 81% of the sample population (33 of the 59 cities, and Athens). Intermediate-period structures lie between 0.20 (Amfissa) and 1.23 (Sparti) times the target (weighted 0.69); only Sparti, Rethymno and Perama, with 1.3% of the population, exceed it.

The Athens urban area averages 1.31 (short-period) and 0.79 (intermediate-period). Its units range from 0.85 (Glyfada) to 2.00 (Perama), so a single point would hide a factor of 2.3 within one zone. On the mean hazard the weighted factors are 1.96 and 0.86: the target is exceeded everywhere for short-period structures and at sites with 24% of the population for intermediate-period ones.

Over the 59 cities and Athens, the highest-to-lowest ratio is 3.3 (short-period) and 6.3 (intermediate-period). Within a zone it reaches 2.9 (short-period, Zone 5) and 4.2 (intermediate-period, Zone 4). Zone averages range only from 1.01 to 1.69, so most of the non-uniformity lies within zones.

Population-weighted geometric means separate the contributions: the shape of the median hazard curve relative to the $k = 3$ power law contributes 1.04 for S_α and 1.14 for S_β, the design fractile 1.00 (by definition) and 0.51 (the effect of the 84th-percentile S_β), and zone averaging 1.14 and 1.15. Moving to the mean hazard multiplies the result by a further 1.63 and 1.25.

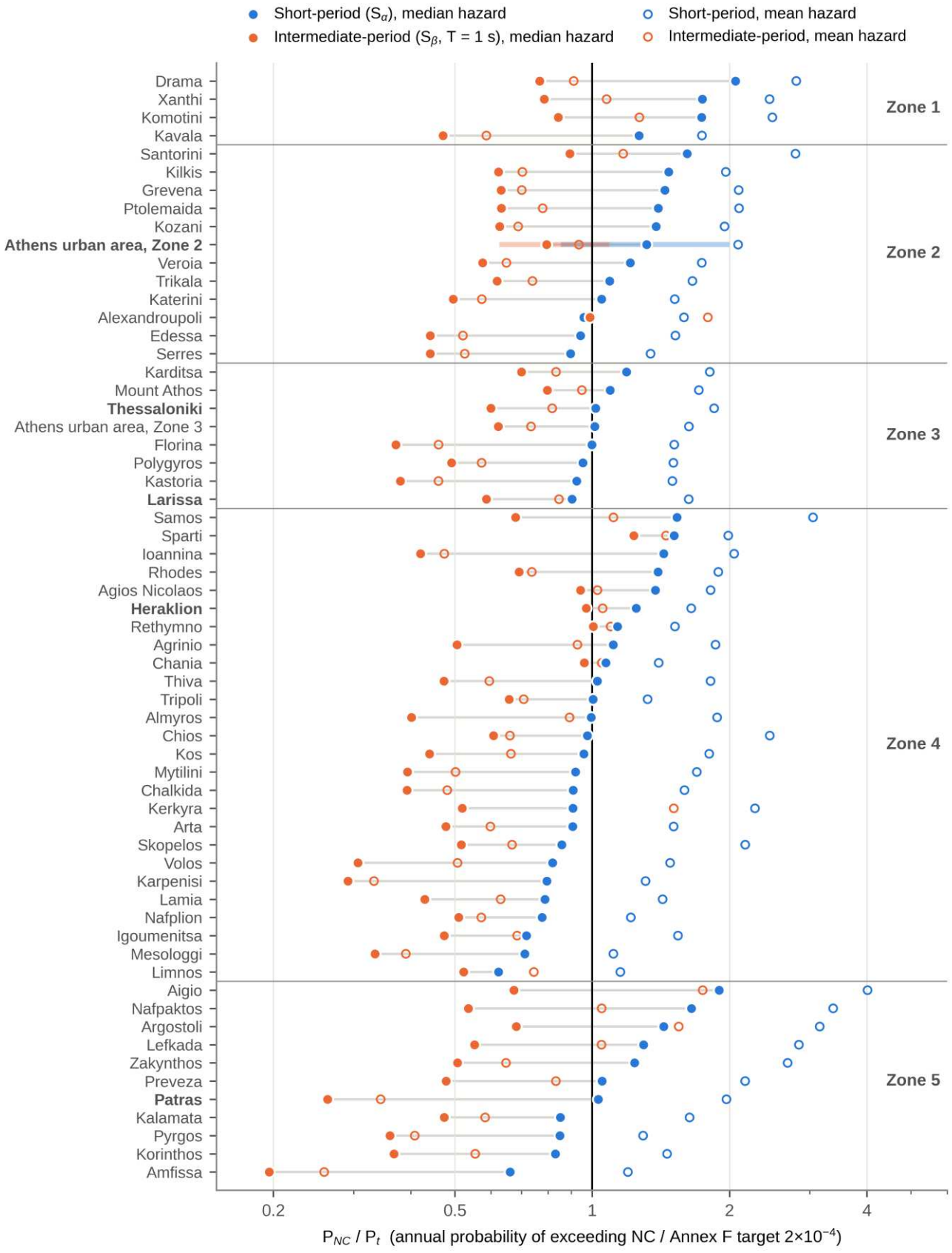


Fig. 1 Ratio of the annual probability of exceeding NC to the Annex F target ($P_t = 2 \times 10^{-4}$/yr) under the proposed zonation, for short-period (S_α) and intermediate-period (S_β, $T = 1$ s) structures, on the ESHM20 median hazard (filled) and mean hazard (open). The Athens urban area is shown as population-weighted means of its units

in Zones 2 and 3; shaded bars give the range over the 53 Zone 2 units (median hazard). Cities with more than 100,000 inhabitants are in bold. Rock, code-calibrated fragility ($m_{EC8} = 2.51$, $\beta = 0.6$)

3.2 Sensitivity to the intensity measure, dispersion and margin

The design plateau is flat from T_B (0.08–0.10 s) to T_C (0.31–0.41 s), whereas the UHS peaks at T_p and decays towards T_C. P_{NC} therefore depends on where T_1 lies (Table 2). On the median hazard, the weighted ratio is 1.06 at 0.10 s, 1.41 at T_p, 0.73 at 0.30 s and 0.61 at T_C. The share of the population above the target falls from 95% at T_p to none at T_C. The S_α construct of Eq. (1) gives 1.21, between the values at 0.10 s and T_p. The construct therefore represents T_1 of about 0.1–0.2 s, and exceedance of the target is a property of structures near the spectral peak, not of the whole plateau. On the mean hazard, the ratio exceeds 1 everywhere up to T_p and falls to 0.80 at T_C. The typical 3–8-storey buildings whose design forces motivated the 84th-percentile S_β (T_1 of about 0.3–0.8 s) lie at 0.61–0.73 times the target on the median hazard (0.30 s, T_C, 0.5 s and 0.75 s in Table 2) and at 0.80–0.97 on the mean, below the Annex F target.

With m_{EC8} recalibrated, changing β from 0.4 to 0.8 moves the short-period ratio from 1.43 to 0.93; with m fixed at 2.51, from 0.59 to 2.46. The absolute level thus depends on the assumed dispersion and margin, but the ranking of the 60 sites (Spearman correlation with the central case 0.91–0.99) and the short/intermediate ratio (1.68–1.81) change little.

Table 2 Sensitivity of the population-weighted P_{NC}/P_t under zone design (main sample). Share: share of the sample population with $P_{NC}/P_t > 1$. Short/intermediate: population-weighted geometric mean of P_{NC}(short-period)/P_{NC}(T = 1 s), with the short-period measure of the row where applicable. Median hazard unless stated.

Case	Short-period P_{NC}/P_t (share)	Intermediate-period P_{NC}/P_t (share)	Short/intermediate
Central: S_α, SA(1.0 s), β = 0.6	1.21 (81%)	0.69 (1%)	1.78
ESHM20 mean hazard	1.96 (100%)	0.86 (24%)	2.33
SA(0.10 s); SA(T_p)	1.06 (51%); 1.41 (95%)	–	1.55; 2.07
SA(0.30 s); SA(T_C)	0.73 (4%); 0.61 (0%)	–	1.08; 0.89
SA(0.5 s); SA(0.75 s) instead of SA(1.0 s)	–	0.68; 0.71	1.80; 1.73
β = 0.4; 0.8, m_{EC8} recalibrated	1.43; 0.93	0.81; 0.55	1.81; 1.73
β = 0.4; 0.8, m = 2.51 fixed	0.59; 2.46	0.34; 1.49	1.80; 1.68
16th; 84th percentile hazard	0.43; 3.43	0.37; 1.40	–

3.3 From hazard tolerance to risk deviation

For a locally power-law hazard curve, P_{NC} scales as θ^{-k}, so changing the design value by a factor $1 + r$ changes P_{NC} by about $(1 + r)^{-k}$. Here k is the hazard slope near the peak of the integrand. Figure 2 confirms this for the ratio of P_{NC} under zone design to that under own-value design, plotted against $r = S_{zone}/S_{own} - 1$:

$$\frac{P_{NC,zone}}{P_{NC,own}} \approx (1+r)^{-k_{eff}} \qquad (5)$$

The effective exponent is fitted over the 59 cities and the Athens urban area (the aggregate of its 53 Zone 2 units). On the median hazard, k_{eff} is 2.73 for S_α and 2.94 for S_β, with residual logarithmic standard deviations of 0.021 and 0.040; on the mean hazard it is 2.22 and 2.46. Sites in Eastern Macedonia and Thrace, whose curves are flatter, lie below the fit.

The thresholds of Pitilakis et al. (2024) map into P_{NC} as follows (S_α, median hazard):

- $\pm 10\%$ corresponds to factors of 1.33 and 0.77;
- $\pm 15\%$ to 1.56 and 0.68;
- $\pm 20\%$ to 1.84 and 0.61.

For S_β the factors are 1.36/0.76, 1.61/0.66 and 1.93/0.59. The ranking of under-protected sites follows the hazard ratios of Pitilakis et al. (2024), with the deviation amplified about 2.7-fold in log terms.

For S_α, r ranges from −24% to +20%. The largest ratios occur at Aigio (2.18), Nafpaktos (1.87), Perama (1.75) and Argostoli (1.73), where r is −17% to −24%; with the published site value of Pitilakis et al. (2024), Aigio's ratio is 1.82 (r = −19.6%). For S_β, which was not checked against site values, r ranges from −44% to +37% and the ratio reaches 6.1 at Aigio, 4.6 at Argostoli, 4.0 at Alexandroupoli and 3.7 at Kerkyra.

Within the Athens urban area, which Pitilakis et al. (2024) checked at one point against the ±10% threshold for their largest cities (r = −9.5%), r_α ranges from −21% (Perama) to +4% across the 55 units, and units holding 35% of its population lie outside ±10%.

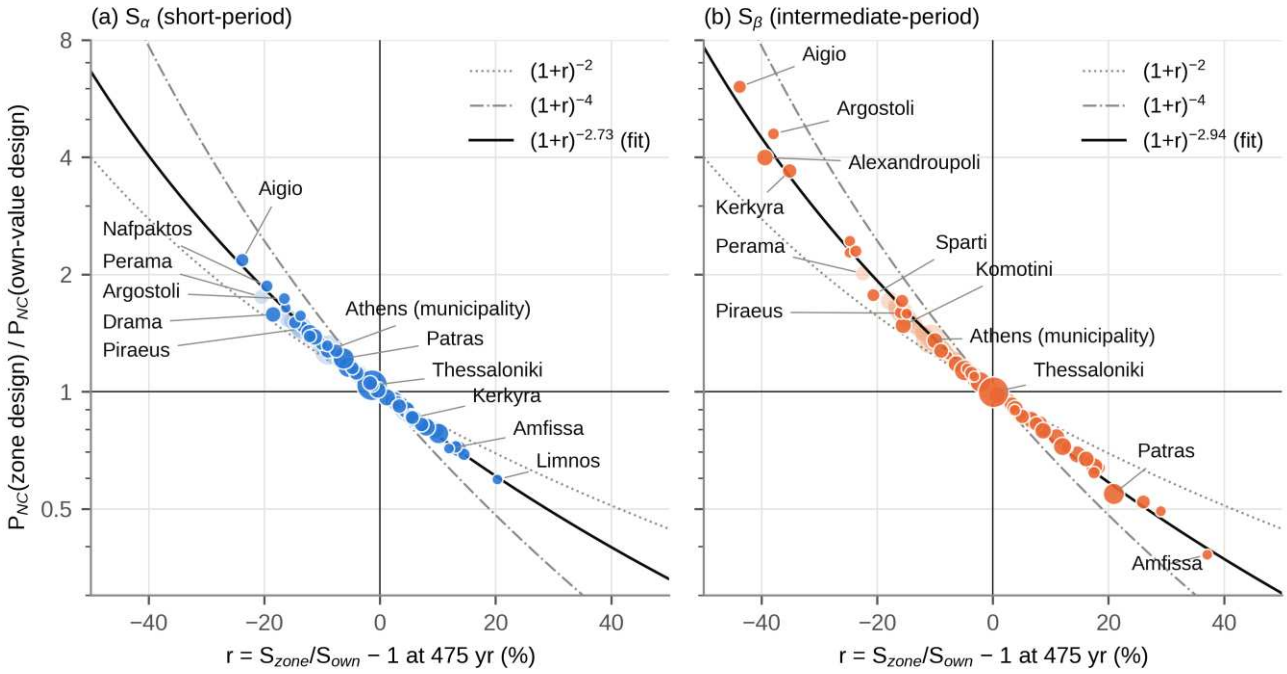


Fig. 2 Ratio of P_{NC} under zone design to that under own-value design against the relative deviation r of the zone value from the site value at 475 years, on the ESHM20 median hazard: (a) short-period, (b) intermediate-period structures. Dark markers: test cities; light markers: units of the Athens urban area. Marker area is proportional to population. Curves: $(1+r)^{-k}$ for k = 2 and 4 and the fitted k_{eff} (59 cities and Athens). $m_{EC8} = 2.51$, $\beta = 0.6$. The label Athens (municipality) marks the Athens municipal unit; the Athens site used in the fit is the aggregate of the 53 Zone 2 units

3.4 Short- versus intermediate-period structures

Under zone design, P_{NC} of short-period structures is 1.78 times that of structures with T = 1 s on the median hazard (population-weighted geometric mean; range 0.97–3.92) and 2.33 times on the mean hazard (Table 2). The ratio is almost unchanged under own-value design with the same percentiles (1.80) but falls to 0.91 with median values for both parameters. The disparity between the S_α construct and T = 1 s is caused by the percentile convention, not by zoning or hazard shape; its variation within the plateau comes from the flat plateau against a decaying UHS. It is largest at the spectral peak (2.11 at SA(T_p), against 1.07 under a single median convention) and disappears towards the end of the plateau (0.89 and 0.77 at each site's own T_C).

A single convention would, however, restore the narrow plateau that led Pitilakis et al. (2024) to the 84th percentile: averaged over the cities of each zone, $T_C = S_\beta T_\beta / S_\alpha$ is 0.23–0.29 s with medians and 0.30–0.40 s with the adopted convention, which widens the plateau by raising S_β only.

3.5 Zone 1 value

At 0.13 g, the population-weighted short-period ratio of the four Zone 1 cities is 1.69, against 1.19 for Zones 2–5 (+42%, median hazard); on the mean hazard the figures are 2.35 and 1.94 (+21%). For intermediate-period structures the excess is 4% (median) and 13% (mean). The hazard curves of Eastern Macedonia and Thrace are flatter at the long return periods that control P_{NC}.

Pitilakis et al. (2024) note that 0.13 g is below the current minimum of 0.16 g and suggest that the authorities consider at least 0.16 g. Scaling the Zone 1 values S_α and S_β by 0.16/0.13 lowers the Zone 1 ratios to 1.09 and 0.44 on the median hazard, 9% and 36% below the other zones (17% and 26% on the mean hazard). This is indicative, since it rests on four cities with 0.21 million inhabitants.

4 Discussion

4.1 Code simplifications

Formula F.5, $P_{NC} \approx \lambda_H(\theta)\exp(k^2\beta^2/2)$ (Cornell et al. 2002), is exact only for a power law. ESHM20 curves in Greece are concave in log–log space; with the tangent slope at θ (2.7–6.1), F.5 overestimates P_{NC} for S_β by a median factor of 3.8 for S_a and 2.7 S_β on the median hazard. Annex F applies F.5 with k at $S_{e,ref}$, which may be mapped in the National Annex. For own-value design, F.5 with $k = 3$ gives 0.55–1.21 times the numerical result, whereas with the site slope at S_{475} (1.6–2.8) it is conservative at all sites (by 5–53%).

EC8-2G derives the performance factor with $k = 3$, $\gamma_{NC} = 1.5 \approx (1600/475)^{1/3}$ for CC2 (4.3(5)). On the median hazard, the NC action $1.5S_{475}$ has a return period of 865–1656 years for S_α (population-weighted 1267) and 1019–1413 years for S_β (1214), varying from site to site within each zone. Because the calibration of Sect. 2.4 already uses γ_{NC}, this effect is included in the results of Sect. 3, not additional to them. Specifying return periods instead would require a separate 1600-year zonation, in which the deviations of Sect. 3.3 would reappear; mapping k is an alternative within the existing zones.

4.2 Implications for the National Annex

1. Acceptance thresholds for the zonation can be expressed in terms of the Annex F target. With $k_{eff} \approx 2.7$ on the median hazard, a hazard tolerance of $\pm\epsilon$ corresponds to P_{NC} factors of about $(1 \mp \epsilon)^{-2.7}$.
2. The S_β zonation deserves the same scrutiny as S_α: Aigio, Argostoli, Alexandroupoli and Kerkyra are 35–44% below their own S_β values.
3. The mixed percentile convention is a policy choice with a quantifiable risk consequence: it makes structures near the spectral peak about twice as likely to exceed NC as intermediate-period ones

(2.1 on the median hazard), while structures near T_C and the 3–8-storey buildings it was meant to serve are at 0.61–0.73 times the target. The issue is the flat plateau against a decaying UHS rather than the level of S_α alone.

4. Whether the target is assessed on the median (as Annex F specifies) or on the mean hazard (the ESHM20 best estimate) changes the short-period result from 1.21 to 1.96. The National Annex may state which applies.

5. Factors on the zone values that would meet the target are given in Table 3. A factor on S_α raises the whole plateau, so it depends on the reference period: on the median hazard and under a population-weighted-mean criterion it is 1.00–1.28 for the S_α construct and 1.06–1.35 at SA(T_p), but 0.70–0.86 at SA(T_C); the S_β factors are 0.71–0.91. A per-site multiplier is approximately $(P_{NC}/P_t)^{1/k_{eff}}$.

Table 3 Factors on the proposed zone values for which the zone meets the Annex F target, under two criteria: population-weighted mean $P_{NC} = P_t$ (first value) and $P_{NC} \leq P_t$ for 90% of the zone population (second value). The factor on S_α is evaluated at three reference periods: the S_α construct (T_1 of about 0.1–0.2 s), the UHS peak T_p and the zone corner period T_C. Main sample; exact numerical solution.

Zone	S_α construct	SA(T_p)	SA(T_C)	S_β
Median hazard				
1	1.28 / 1.37	1.35 / 1.45	0.83 / 0.90	0.86 / 0.93
2	1.10 / 1.20	1.17 / 1.27	0.86 / 0.93	0.91 / 0.98
3	1.00 / 1.01	1.06 / 1.06	0.83 / 0.83	0.81 / 0.83
4	1.03 / 1.13	1.09 / 1.20	0.76 / 0.83	0.83 / 0.99
5	1.02 / 1.13	1.09 / 1.21	0.70 / 0.82	0.71 / 0.82
Mean hazard				
1	1.57 / 1.70	1.67 / 1.80	0.94 / 1.07	0.98 / 1.14
2	1.37 / 1.49	1.46 / 1.58	0.94 / 1.02	0.97 / 1.04
3	1.30 / 1.32	1.38 / 1.40	0.93 / 0.95	0.91 / 0.93
4	1.25 / 1.36	1.32 / 1.43	0.84 / 0.97	0.91 / 1.04
5	1.35 / 1.58	1.41 / 1.60	0.82 / 1.05	0.81 / 1.02

4.3 Limitations

The fragility is generic: one lognormal shape (β = 0.6) for all periods, representing a structure that just meets the target under the code's hazard assumptions rather than a specific typology. Real buildings carry additional overstrength (Baltzopoulos et al. 2024; Spillatura et al. 2023), and NC exceedance precedes collapse. In the force-based approach strength is verified at SD (EN 1998-1-1, 6.1(3)) and NC is only implied (4.5.1(1), Note 1), so the NC-anchored fragility represents displacement-based design most directly. The analysis is for rock and fixed T_1, at the sites where the zonation was accepted; non-uniformity over the full grid is likely to be larger.

5 Conclusions

The proposed five-zone EC8-2G zonation of Greece was checked against the Annex F target for NC in CC2 at the 59 test cities of the zonation and the 55 units of the Athens urban area, with a fragility calibrated so that the target is met exactly at a site whose median hazard follows the code's $k = 3$ power law.

1. On the median hazard of Annex F, structures with T_1 of about 0.1–0.2 s designed to the zone values lie at 0.62–2.06 times the target (population-weighted 1.21) and structures with $T = 1$ s at 0.20–1.23 (0.69). On the ESHM20 mean hazard the factors are 1.96 and 0.86. The variation is mainly within zones.
2. Within the plateau, P_{NC} decreases from 1.41 times the target at the spectral peak to 0.61 at T_C. Exceedance of the target concerns structures near the peak; typical 3–8-storey buildings (T_1 = 0.3–0.8 s) lie at 0.61–0.73.
3. Zone averaging changes P_{NC} as $(1 + r)^{-k_{eff}}$, with k_{eff} = 2.7–2.9 on the median hazard; the ±20% tolerance of the zonation corresponds to factors of 1.8 and 0.61. Within Athens, units holding 35% of its population deviate from the zone S_α by more than the ±10% applied to the city as a whole. The S_β zonation deviates more, by −44% to +37%.
4. The combination of median S_α and 84th-percentile S_β makes structures near the spectral peak about twice as likely to exceed NC as intermediate-period ones (2.1 on the median hazard, against 1.1 under a single convention); towards T_C the ratio falls below 1 under either convention.
5. Zone 1 at 0.13 g departs most from the target for short-period structures (42% above the other zones on the median hazard). Retaining 0.16 g, an option Pitilakis et al. (2024) themselves raise, would place it 9% below them.
6. Zone factors that would meet the target are given for two criteria and three reference periods; above 1 near the spectral peak, they fall below 1 at T_C.

These results do not question the hazard basis of the proposal. They complement it with a reliability check against the target of EC8-2G itself, while the National Annex is still under consideration.

Acknowledgements

ESHM20 hazard results were obtained from the European Facility for Earthquake Hazard and Risk (EFEHR) under a CC BY 4.0 licence.

Statements and Declarations

- **Funding:** The author declares that no funds, grants, or other support were received during the preparation of this manuscript.

- **Competing interests:** The author declares no competing interests. The views expressed are those of the author and do not necessarily reflect those of Archirodon N.V.
- **Data availability:** ESHM20 hazard curves are available from EFEHR (https://efehr-services.ethz.ch/hazard/api/docs). Population data are from ELSTAT. The site table, zone assignments, interpolated hazard curves and risk results are provided in Online Resource 1.
- **Code availability:** Scripts are available from the author on reasonable request.
- **Author contributions:** The author conceived the study, performed the analysis and wrote the manuscript.
- **Use of AI tools:** Claude (Anthropic) was used to assist in writing and debugging the Python scripts for data retrieval, interpolation, numerical integration and figure generation, and in organizing the data and the supplementary spreadsheet. The author specified the methods, verified the scripts and their results, and takes full responsibility for the content.

Supplementary information

Online Resource 1 (xlsx): site table for 154 sites (including 40 units of the rest of Attica outside the main sample) with zone assignments, population and 475-year site values; P_NC/P_t for all cases on the median and mean hazard, including the dispersion and margin sensitivity and the Zone 1 value of 0.16 g; fractile results; exact and approximate multipliers; zone factors at three reference periods for S_α and for S_β; corner-period cases; closed-form comparisons; and the four-node spread at Aigio, Nafpaktos, Argostoli, Athens and Patras. A README sheet defines every column.

References

Baltzopoulos G, Grella A, Iervolino I (2024) Some issues in the practical application of risk-targeted ground motions. Earthq Eng Struct Dyn 53(3):997–1005. https://doi.org/10.1002/eqe.4058

CEN (2024) EN 1998-1-1:2024. Eurocode 8 – Design of structures for earthquake resistance – Part 1-1: General rules and seismic action. European Committee for Standardization, Brussels.

Cornell CA, Jalayer F, Hamburger RO, Foutch DA (2002) Probabilistic basis for 2000 SAC Federal Emergency Management Agency steel moment frame guidelines. J Struct Eng 128(4):526–533. https://doi.org/10.1061/(ASCE)0733-9445(2002)128:4(526)

Danciu L, Nandan S, Reyes C, Basili R, Weatherill G, Beauval C, Rovida A, Vilanova S, Sesetyan K, Bard P-Y, Cotton F, Wiemer S, Giardini D (2021) The 2020 update of the European Seismic Hazard Model: model overview. EFEHR Technical Report 001, v1.0.0. https://doi.org/10.12686/a15

Danciu L, Giardini D, Weatherill G, et al (2024) The 2020 European Seismic Hazard Model: overview and results. Nat Hazards Earth Syst Sci 24(9):3049–3073. https://doi.org/10.5194/nhess-24-3049-2024

Douglas J, Ulrich T, Negulescu C (2013) Risk-targeted seismic design maps for mainland France. Nat Hazards 65(3):1999–2013. https://doi.org/10.1007/s11069-012-0460-6

EAK (2003) Greek Seismic Code EAK 2003. Earthquake Planning and Protection Organization (OASP), Athens.

Franchin P, Noto F (2023) Reliability-based partial factors for seismic design and assessment consistent with second-generation Eurocode 8. Earthq Eng Struct Dyn 52(13):4026–4047. https://doi.org/10.1002/eqe.3840

Gkimprixis A, Tubaldi E, Douglas J (2019) Comparison of methods to develop risk-targeted seismic design maps. Bull Earthq Eng 17:3727–3752. https://doi.org/10.1007/s10518-019-00629-w

Hellenic Statistical Authority (2023) 2021 Population–Housing Census: permanent population by municipal community. ELSTAT, Piraeus. https://www.statistics.gr/en/2021-census-pop-hous. Accessed July 2026

Labbé P, Paolucci R (2022) Developments relating to seismic action in the Eurocode 8 of next generation. In: Vacareanu R, Ionescu C (eds) Progresses in European Earthquake Engineering and Seismology. 3ECEES, Bucharest 2022. Springer, Cham, pp 26–46. https://doi.org/10.1007/978-3-031-15104-0_2

Luco N, Ellingwood BR, Hamburger RO, et al (2007) Risk-targeted versus current seismic design maps for the conterminous United States. In: Proceedings of the 2007 SEAOC Convention, Lake Tahoe, CA

Monti G, Demartino C, Gardoni P (2023) Towards risk-targeted seismic hazard models for Europe. Sci Rep 13:10717. https://doi.org/10.1038/s41598-023-36947-y

Pitilakis K, Riga E, Apostolaki S, Danciu L (2024) Seismic hazard zonation map and definition of seismic actions for Greece in the context of the ongoing revision of EC8. Bull Earthq Eng 22:3753–3792. https://doi.org/10.1007/s10518-024-01919-8

Silva V, Crowley H, Bazzurro P (2016) Exploring risk-targeted hazard maps for Europe. Earthq Spectra 32(2):1165–1186. https://doi.org/10.1193/112514EQS198M

Spillatura: "Spillatura A, Vamvatsikos D, Kohrangi M, Bazzurro P (2023) Harmonizing seismic performance via risk targeted spectra: state of the art, dependencies, and implementation proposals. Earthq Eng Struct Dyn 52:4277–4299. https://doi.org/10.1002/eqe.3941

Žižmond J, Dolšek M (2019) Formulation of risk-targeted seismic action for the force-based seismic design of structures. Earthq Eng Struct Dyn 48(12):1406–1428. https://doi.org/10.1002/eqe.3206

Supplementary Files

This is a list of supplementary files associated with this preprint. Click to download.

- ESM1.xlsx